Ultrasmall Single-Crystal Indium Antimonide Nanowires

ARTICLE *in* CRYSTAL GROWTH & DESIGN · MAY 2010

Impact Factor: 4.89 · DOI: 10.1021/cg100376u

DOI: 10.1021/cg100376u

CRYSTAL GROWTH & DESIGN
Communication
2010, Vol. 10
2479–2482

Ultrasmall Single-Crystal Indium Antimonide Nanowires

Xunyu Yang, Gongming Wang, Peter Slattery, Jin Z. Zhang, and Yat Li*

Department of Chemistry and Biochemistry, University of California, Santa Cruz, California 95064

Received March 21, 2010; Revised Manuscript Received May 1, 2010

ABSTRACT: We report the rational synthesis of ultrasmall indium antimonide (InSb) nanowires down to 4.5 nm diameter. To achieve uniform InSb nanowires, we designed and performed the synthesis via a vapor−liquid−solid growth mechanism, where monodispersed gold colloids were used as a catalyst. The growth was carried out in a home-built three-zone chemical vapor deposition system, which allows continuous tunability of respective indium and antimony vapor pressure via separate temperature control. Several parameters are important for achieving successful nanowire growth, including the use of catalysts and tuning of the V/III ratio. Scanning electron microscopy revealed that InSb nanowires had uniform diameters with lengths up to several micrometers, and their sizes were defined by gold nanoparticles. High-resolution transmission electron microscopy structural characterization showed that as-prepared InSb nanowires were single crystals elongating along the ⟨111⟩ direction, regardless of wire diameter. Their chemical compositions were characterized by Raman spectroscopy and electron energy loss spectroscopy. The ability to rationally prepare ultrasmall, single-crystal InSb nanowires opens up new opportunities for studying the size-associated fundamental properties and provides insights for potential nanodevice applications.

There is growing interest in indium antimonide (InSb) nanowires due to their unique material properties for functional devices. For instance, InSb material has the smallest bandgap of 0.17 eV[1] and effective mass of $0.0135m_0$[2] among III−V semiconductors, very high electron mobility of 7.8×10^4 cm^2 V^{-1} S^{-1} at room temperature,[3] and large Bohr exciton radius of 54 nm.[4] These properties make InSb a promising candidate for a wide range of device applications, including high speed field-effect transistors,[3] magnetic sensors,[5] infrared detectors,[6] thermoelectric power generation, and cooling devices.[7,8] One-dimensional (1D) nanowires have attracted much attention recently because of their size-associated quantum confinement effect, good vectorial transport properties, and large surface area.[9] In addition, the unique vapor−liquid−solid (VLS) approach allows the growth of single-crystal, dislocation-free nanowires on diverse substrates, even with a large lattice mismatch.[10−12] Importantly, their diameter and electronic properties can be controlled during synthesis in a predictable manner.[9,13,14]

Many physical properties of 1D nanostructures are diameter dependent, and thus they offer a unique opportunity to decouple the interdependence of these properties by varying the diameter. For example, phonons typically have a longer mean free path than electrons in materials, and thus the scattering for phonons will be more efficient than electrons in a nanostructure when its size is comparable to or smaller than the mean free path of phonon.[15−17] In this regard, 1D nanowires afford great potential to address fundamental scientific issues in technology, such as thermoelectric energy conversion by decoupling the thermal conductivity and electrical conductivity, which remains very challenging for bulk or planar materials. Recent studies have demonstrated that rough silicon nanowires with a diameter of ∼50 nm show a 100-fold reduction in thermal conductivity compared to bulk silicon, yielding a dimensionless thermoelectric figure of merit (ZT) of 0.6 at room temperature.[18] The enhancement of ZT is due to the reduction of heat transport via phonons. While bulk InSb has a ZT of 0.6 at temperature of 673 K,[7] low-dimensional InSb nanowires are predicted to have ZT > 1 as the diameter of nanowire decreased.[19] However, in order to achieve ZT ∼ 3 at room temperature for practical applications, theoretical calculations suggested ultrasmall InSb nanowires with a diameter below 30 nm are necessary.[19] Yet, the controlled growth of InSb nanowire less than 30 nm has not been reported. To address this issue, here we present a new and simple approach for synthesizing single-crystal, ultrasmall InSb nanowires with diameters down to ∼4.5 nm. The ability to prepare molecular-scale, single-crystal InSb nanowires opens up new opportunities for studying the size associated physical properties and nanodevice applications.

To date, few experimental studies have been reported on the rational growth of InSb nanowires. One common method to prepare InSb nanowires is electrochemical deposition in porous anodic aluminum oxide templates,[20,21] but it is challenging to achieve ultrathin nanowires (e.g., < 30 nm) as the diameter is determined by the pore size of the template. On the other hand, synthesis of InSb nanowires using a metal nanocluster-mediated VLS method has the potential to overcome this limitation for producing ultrasmall nanostructures, whereas the nanowire diameter is controlled by the size of the nanoparticle. Indeed, VLS growth of InSb nanowires using InSb as the source have been demonstrated on Si substrate,[22,23] InSb substrate in a closed quartz tube,[24] or on SiO_2 substrate via direct antimonidization of molten indium.[25,26] These previous studies suggested that the indium-rich condition is indispensable during the nucleation stage of InSb nanowire growth via a VLS mechanism.[25,26] For example, Ye et al. coated the growth substrate with indium film in order to increase the indium vapor pressure;[25,26] however, it is technically challenging to tune the V/III ratio by heating the InSb source in a conventional single-zone chemical vapor deposition (CVD). The V/III ratio is known to be an important parameter for growing III−V semiconductors.[27−29] The recent demonstration of CVD growth of InSb nanowire showed that the V/III ratio can affect the chemical stoichiometry and thereby the material properties of InSb.[23] The preliminary experiments on nanowire growth using InSb powder as a precursor resulted in the growth of antimony or antimony oxide nanowires. Elemental analysis showed that the InSb source turned into indium-rich material after the growth, which suggests the partial vapor pressure of In is lower than Sb during the growth.

To overcome the above issue, we employed the three-zone CVD system that allows separate control of two key growth parameters, the substrate temperature and the individual source temperature (Figure 1). The ability to tune the In and Sb source temperature independently allows control over the ratio of V/III vapor pressure. In addition, our synthetic strategy allows us to use

*Corresponding author. E-mail: yli@chemistry.ucsc.edu.

Published on Web 05/11/2010

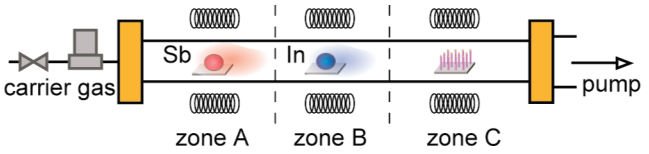

Figure 1. Schematic shows the three-zone CVD for the growth of InSb nanowires, in which the source temperature and substrate temperature can be separately adjusted. The Sb powder and In ingot were used as precursor sources and placed into upstream zone A and B. Growth substrate coated with gold nanoparticles was placed in downstream zone C.

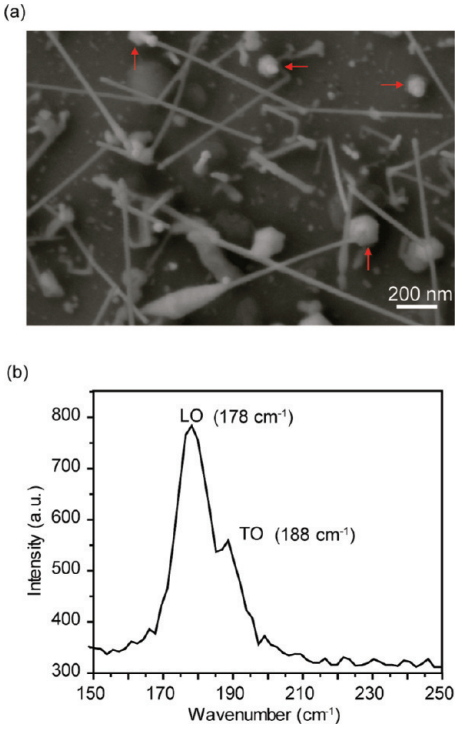

Figure 2. (a) SEM images of InSb nanowires grown on InSb(100) substrate using 30 nm gold nanoparticles as catalyst. The red arrows highlight the crystal base for the nanowire growth. (b) Raman spectrum collected from ensemble of InSb nanowires grown on SiO_2 substrate.

inexpensive Sb metal powder and In ingot as precursors (vs metal−organic sources or InSb material), which were respectively placed in zone A and zone B upstream (Figure 1). The partial vapor pressures of In and Sb were initially adjusted to be ca. 6×10^{-3} Torr with a V/III ratio of approximately 1:1,[30,31] by setting the source temperatures to 900 °C (zone A) and 530 °C (zone B). The growth substrate coated with gold colloids was placed in zone C downstream. Under these conditions, nanowire growth was observed on SiO_2 and InSb(100) substrates in the temperature range from 400 to 480 °C, in hydrogen at a pressure of 150 Torr. We did not observe a significant difference in morphology or yield of nanowire under these growth conditions. The successful growth of InSb nanowire requires critical exclusion of even trace amounts of impurities in CVD, such as oxygen. Since In and Sb have similar electronegativity and a low bond energy, the presence of residual oxygen in CVD will impose a strong competition with In and Sb for the formation of oxide materials.

Scanning electron microscopy (SEM) images revealed that as-grown InSb nanowires had uniform morphology, and the lengths of the nanowires were 300 nm to 1 μm (Figure 2a). Au nanoparticles were observed at the tip of nanowires, confirming a nanocluster-mediated VLS growth mechanism and the nanowire

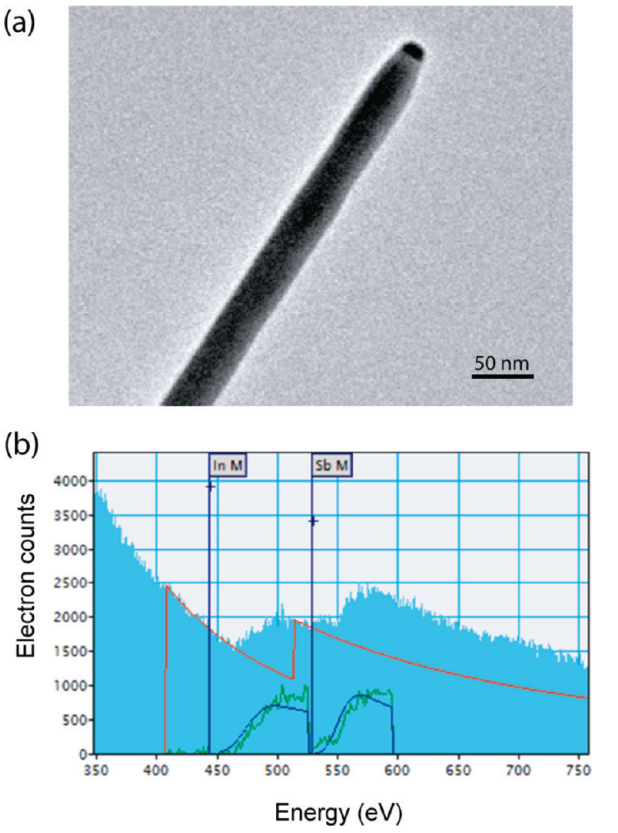

Figure 3. (a) Bright-field TEM image of a 30-nm InSb nanowire; (b) EELS spectrum collected from a single 10-nm InSb nanowire. The blue profile is the experimental result. The red curve highlights the background profile. The green lines are In M and Sb M edge signal after the subtraction of the experimental profile and the background signal. The blue lines are simulated In M and Sb M edge peaks.

diameters are determined by the size of gold colloids. Figure 2a shows the nanowires obtained using 30 nm gold colloids as the catalyst. We also obtained InSb nanowires with similar morphology on SiO_2 substrates (see Figure S1, Supporting Information), suggesting the substrate may not significantly impact the growth mechanism. Most of the InSb nanowires were observed to grow from a crystal base (highlighted with red arrows in Figure 2a), consistent with previous reports of InSb[32] and other III-antimonide nanowires.[25] By using a smaller size of Au colloids as catalysts, we were able to obtain nanowires with diameters down to ~4.5 nm.

Raman spectrum (Figure 2b) of the ensemble InSb nanowires on SiO_2 substrate showed two peaks, 178 and 188 cm^{-1}, which were associated with the transverse and longitudinal mode of InSb, respectively.[25] In comparison to the characteristic Raman peaks of bulk InSb, 180 and 190 cm^{-1},[33] these Raman peaks are slightly shifted to a lower wavenumber, likely due to a laser-induced heating effect.[34−36] These data, together with the electron energy loss spectroscopy (EELS) characterization to be discussed in the following, confirmed the chemical composition of as-prepared nanowires as InSb.

Bright-field TEM image of a representative 30 nm diameter InSb nanowire (Figure 3a) shows that the nanowire was uniform and free of dislocations. Au nanoparticle was observed on the nanowire tip as expected for the VLS process. The nanowire diameter was slightly larger than the Au nanoparticle, suggesting that slight lateral coating on the nanowires may have occurred. To quantitatively determine the chemical composition of the nanowires, we carried out EELS on individual InSb nanowires. Figure 3b shows the EELS spectrum collected from a typical 10-nm-diameter InSb nanowire. By subtracting the background

signal (red curve), we observed two strong peaks (green curve) with onset energies of 443 and 528 eV, corresponding to the characteristic energy loss of In M and Sb M edges, respectively. The elemental composition of the InSb nanowire was calculated by fitting the experimental profiles with the simulated curve (blue). These data indicate that the nanowire contains In and Sb with an approximately 5.5:4.5 atomic ratio. In addition, energy dispersive X-ray spectroscopy studies also confirm that the nanoparticle at the nanowire tip was composed of 87% of gold, 8% of In, and 5% of Sb, (see Figure S2, Supporting Information), confirming the activity of Au−In−Sb ternary alloys in the catalyzed growth.

In comparison to other reported CVD growth of InSb nanowires,[24−26] our method offers distinct tunability of the V/III ratio and substrate temperature in a wider range. To understand the effect of the V/III ratio on the growth of InSb nanowires, we systematically varied the In and Sb source temperature, while keeping the substrate temperature at 400 °C and growth pressure at 150 Torr. The results were illustrated in Figure S3, Supporting Information. We observed InSb nanowire growth from a broad range of V/III ratios, from 0.0125 (zone A: 900 °C; zone B: 410 °C) to 10 (zone A: 900 °C; zone B: 600 °C). Outside this growth window, only InSb particles could be achieved. Importantly, the results revealed that a slightly Sb-rich condition (V/III vapor pressure of 2:1) would favor the growth of uniform and long InSb nanowires, in contrast to the previous studies. At In-rich conditions, tapered and short InSb nanowires were the main product.

High-resolution TEM was used to characterize the structural details of InSb nanowires. Representative lattice-resolved TEM images obtained from 4.5, 9, and 19 nm diameter InSb nanowires (Figure 4) show that the nanowires were dislocation-free single crystals. These ultrasmall InSb nanowires had a thin amorphous oxide layer of ca. 3−5 nm, which is commonly observed in InSb.[37] Interestingly, we observed that the amorphous layer turned into polycrystalline quantum structures under a strong electron beam during imaging (see Figure S4, Supporting Information). By analyzing the crystal structure, we believe that polycrystalline structures were antimony oxide. The growth directions of these InSb nanowires were analyzed based on the lattice-resolved TEM images. In Figure 4a,b showing sub-10-nm-nanowires, the lattice fringes were perpendicular to the growth axis of InSb nanowire with a measured lattice spacing of 3.71 and 3.74 Å, respectively. These values are consistent with the *d*-spacing of the {111} plane of InSb (3.74 Å) with zinc blende crystal structure, indicating the nanowires were zinc blende InSb growing along the ⟨111⟩ direction. For Figure 4c, the measured lattice spacing of 3.86 Å is equivalent to the *d*-spacing of the {3/2 1/2 1/2} plane of InSb. In addition, the angle measured between the lattice fringes and the nanowire growth axis was ∼80 deg (Figure 4c), which is consistent with a theoretical value between the (111) plane and $(3\bar{1}\bar{1})$ plane of zinc blende InSb. These data confirmed that the growth direction of 20 nm InSb nanowire is ⟨111⟩ as well. We observed the same growth direction in all InSb nanowires we studied, including nanowires with a larger diameter (see Figure S5, Supporting Information), indicating that the growth preference is not determined by nanowire diameter as found in silicon nanowires.[38] The InSb nanowires were not aligned at a angle of approximately 35 deg with the InSb(100) substrate could be due to the oxide layer on InSb substrate and the formation of crystal base during the growth.

In summary, we have demonstrated, for the first time, the controlled growth of ultrasmall InSb nanowires down to the sub-5-nm scale. We attribute the successful growth of these nanowires to several key factors. First, is the ability to adjust the temperature of the In and Sb sources (and thereby In and Sb vapor pressure) and the substrate separately. A growth window for InSb nanowires, with substrate temperature 400−480 °C and the V/III vapor pressure from 0.0125 to 10, was discovered in our system, Second, the use of monodispersed Au colloidal particles is

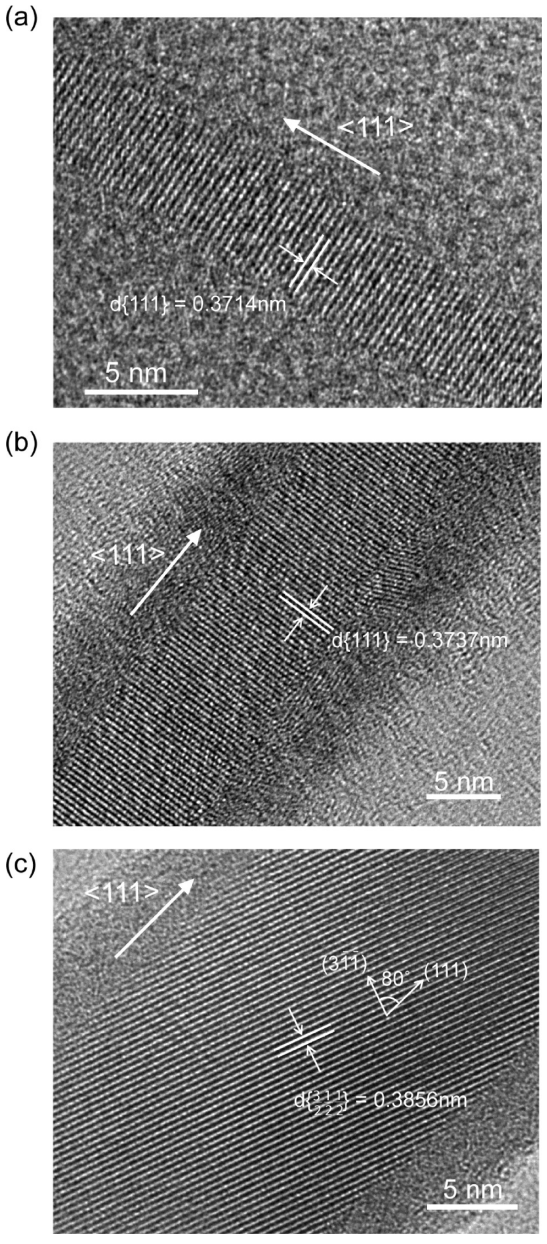

Figure 4. Lattice-resolved TEM images of single crystal InSb nanowires, with a diameter of (a) 4.5 nm; (b) 9 nm; and (c) 19 nm. The white lines indicate the measured *d*-spacings, and the white arrows highlight the ⟨111⟩ growth directions of nanowires.

indispensable for preparing nanowires with desired diameters. Finally, to avoid the formation of oxide materials, it is critical to remove the residual oxygen and avoid air diffusion into the CVD system during synthesis. TEM studies show that the InSb nanowires synthesized by our approach are single-crystal, dislocation-free structures, with a diameter tuned down to 4.5 nm. All InSb nanowires grow along the ⟨111⟩ direction in the diameter range of 4.5−30 nm studied. The ability to design and prepare ultrasmall InSb nanowires provides new opportunities for studying the quantum confinement effect on thermoelectric properties of a potentially high ZT material as a function of wire diameter and thermoelectric device applications.

Acknowledgment. The authors acknowledge support from UCSC (Special Research Grant) and UCEI Award SC-08-93. J.Z.Z. is grateful to the BES Division of the US DOE and NSF for financial support. The SEM and TEM works were performed at

Molecular Foundry and NCEM at Lawrence Berkeley National Laboratory, which are supported by the Office of Science, Office of Basic Energy Sciences of the U.S. Department of Energy under Contract No. DE-AC02-05CH11231. We thank Fang Qian for helpful discussions. We acknowledge Q. Ramasse and C. Y. Song for helpful discussion on TEM studies.

Supporting Information Available: SEM and TEM microscopy data, and EDX spectroscopy data. This information is available free of charge via the Internet at http://pubs.acs.org/.

References

(1) Madelung, O. *Data in Science and Technology, Semiconductors Group IV Elements and III-V Compounds*; Springer: Berlin, 1991; p 141.
(2) Vurgaftman, I.; Meyer, J. R.; Ram-Mohan, L. R. *J. Appl. Phys.* **2001**, *89*, 5815–5875.
(3) Ashley, T.; Dean, A. B.; Elliott, C. T.; Pryce, G. J.; Johnson, A. D.; Willis, H. *Appl. Phys. Lett*. **1995**, *66*, 481.
(4) Wise, F. W. *Acc. Chem. Res.* **2000**, *33*, 773.
(5) Heremans, J. *J. Phys. D: Appl. Phys.* **1993**, *26*, 1149.
(6) Zhang, Y. X.; Williamson, F. O. *Appl. Opt*. **1982**, *21*, 2036.
(7) Yamaguchi, S.; Matsumoto, T.; Yamazaki, J.; Kaiwa, N.; Yamamoto, A. *Appl. Phys. Lett*. **2005**, *87*, 201902.
(8) Seol, J. H.; Moore, A. L.; Saha, S. K.; Zhou, F.; Shi, L.; Ye, Q.; Scheffler, R. H.; Mingo, N.; Yamada, T. *J. Appl. Phys*. **2007**, *101*, 023706.
(9) Li, Y.; Qian, F.; Xiang, J.; Lieber, C. M. *Mater. Today* **2006**, *9*, 18.
(10) Qian, F.; Gradecak, S.; Li, Y.; Wen, C. Y.; Lieber, C. M. *Nano Lett*. **2005**, *5*, 2287.
(11) Qian, F.; Li, Y.; Gradecak, S.; Park, H. G.; Dong, Y.; Ding, Y.; Wang, Z. L.; Lieber, C. M. *Nat. Mater*. **2008**, *7*, 701.
(12) Qian, F.; Li, Y.; Gradecak, S.; Wang, D.; Barrelet, C. J.; Lieber, C. M. *Nano Lett*. **2004**, *4*, 1975.
(13) Wagner, R. S.; Ellis, W. C. *Appl. Phys. Lett*. **1964**, *4*, 89.
(14) Hu, J.; Odom, T. W.; Lieber, C. M. *Acc. Chem. Res*. **1999**, *32*, 435.
(15) Seyler, J.; Wybourne, M. N. *J. Phys.: Condens. Matter* **1990**, 8853.
(16) Higgins, J. M.; Schmitt, A. L.; Guzei, I. A.; Jin, S. *J. Am. Chem. Soc*. **2008**, *130*, 16086.
(17) Zhou, F.; Szczech, J.; Pettes, M. T.; Moore, A. L.; Jin, S.; Shi, L. *Nano Lett*. **2007**, *7*, 1649.
(18) Hochbaum, A. I.; Chen, R.; Delgado, R. D.; Liang, W.; Garnett, E. C.; Najarian, M.; Majumdar, A.; Yang, P. *Nature* **2007**, *451*, 163.
(19) Mingo, N. *Appl. Phys. Lett*. **2004**, *84*, 2652.
(20) Yang, Y.; Li, L.; Huang, X.; Li, G.; Zhang, L. *J. Mater. Sci*. **2007**, *42*, 2753.
(21) Khan, M. I.; Wang, X.; Bozhilov, K. N.; Ozkan, C. S. *J. Nanomater*. **2008**, *2008*, 698759.
(22) Zhou, J. F.; Chen, Z.; He, L. B.; Xu, C. H.; Yang, L.; Han, M.; Wang, G. H. *Eur. Phys. J. D*. **2007**, *43*, 283.
(23) Zhou, F.; Moore, A. L.; Petter, M. T.; Lee, Y.; Seol, J. H.; Ye, Q. L.; Rabenberg, L.; Shi, L. *J. Phys. D: Appl. Phys*. **2010**, *43*, 025406.
(24) Park, H. D.; Prokes, S. M.; Twigg, M. E.; Ding, Y.; Wang, Z. L. *J. Cryst. Growth* **2007**, *304*, 399.
(25) Vaddiraju, S.; Sunkara, M. K.; Chin, A. H.; Ning, C. Z.; Dholakia, G. R.; Meyyappan, M. *J. Phys. Chem. C* **2007**, *111*, 7339–7347.
(26) Ye, Q.; Yamada, T.; Liu, H.; Scheffler, R. H.; Mingo, N.; Leverenz, R. L. *Mater. Res. Soc. Symp. Proc*. **2006**, *940E*, 75.
(27) Dick, K. A.; Caroff, P.; Bolinsson, J.; Messing, M. E.; Johansson, J.; Deppert, K.; Wallenberg, L. R.; Samuelson, L. *Semicond. Sci. Technol*. **2010**, *25*, 024009.
(28) Dayeh, S. A.; Yu, E. T.; Wang, D. *Nano Lett*. **2007**, *7*, 2486.
(29) Caroff, P.; Wagner, J. B.; Dick, K. A.; Nilsson, H. A.; Jeppson, M.; Deppert, K.; Samuelson, L.; Wallenberg, L. R.; Wernersson, L. *Small* **2008**, *4*, 878.
(30) Rosenblatt, G. M.; Birchenall, C. E. *J. Chem. Phys*. **1961**, *35* (3), 788.
(31) Geiger, F.; Busse, C. A.; Loehrke, R. I. *Int. J. Thermophys*. **1987**, *8* (4), 425.
(32) Caroff, P.; Messing, M. E.; Borg, B. M.; Dick, K. A.; Deppert, K.; Wernersson, L. *J. Phys. D: Appl. Phys*. **2009**, *43*, 025406.
(33) Aoki, K.; Anastassakis, E.; Cardona, M. *Phys. Rev. B* **1984**, *30* (2), 681.
(34) Piscanec, S.; Cantoro, M.; Ferrari, A. C.; Zapien, J. A.; Lifeshitz, Y.; Lee, S. T.; Hofmann, S.; Robertson, J. *Phy. Rev. B* **2003**, *68*, 241312.
(35) Gupta, R.; Xiong, Q.; Adu, C. K.; Kim, U. J.; Eklund, P. C. *Nano Lett*. **2003**, *3*, 627.
(36) Adu, K. W.; Gutierrez, H. R.; Kim, U. J.; Sumanasekera, G. U.; Eklund, P. C. *Nano Lett*. **2005**, *5*, 409.
(37) Tang, X.; van Welzenis, R. G.; van Setten, F. M.; Bosch, A. J. *Semicond. Sci. Technol*. **1986**, *1*, 355.
(38) Wu, Y.; Cui, Y.; Huynh, L.; Barrelet, C. J.; Bell, D. C.; Lieber, C. M. *Nano Lett*. **2004**, *4* (3), 433.